Biosensors and Bioelectronics 90 (2017) 410–417

Contents lists available at ScienceDirect

Biosensors and Bioelectronics

journal homepage: www.elsevier.com/locate/bios

ARM-microcontroller based portable nitrite electrochemical analyzer using cytochrome *c* reductase biofunctionalized onto screen printed carbon electrode

Paulraj Santharaman[a], Krishna Arun Venkatesh[b], Kanagavel Vairamani[b], Alby Robson Benjamin[c], Niroj K. Sethy[d], Kalpana Bhargava[d], Chandran Karunakaran[a,*]

[a] *Biomedical Research Laboratory, Department of Chemistry, VHNSN College (Autonomous), Virudhunagar 626 001, Tamil Nadu, India*
[b] *University Science Instrumentation Centre (USIC), Madurai Kamaraj University, Madurai 625 021, Tamil Nadu, India*
[c] *Department of Physics, The American College, Madurai 625 002, Tamil Nadu, India*
[d] *Peptide and Proteomics Division, Defence Institute of Physiology & Allied Sciences, Defence Research and Development Organisation, Timarpur, Delhi 110 054, India*

ARTICLE INFO

Keywords:
Cytochrome c reductase
Biofunctionalization
Covalent coupling
ARM microcontroller
Nitrite
Cardiac cells

ABSTRACT

Nitrite (NO_2^-) supplementation limits hypoxia-induced oxidative stress and activates the alternate NO pathway which may partially account for the nitrite-mediated cardioprotection. So, sensitive and selective biosensors with point-of-care devices need to be explored to detect the physiological nitrite level due to its important role in human pathophysiology. In this work, cytochrome *c* reductase (CcR) biofunctionalized self assembled monolayer (SAM) functionalized on gold nanoparticles (GNPs) in polypyrrole (PPy) nanocomposite onto the screen printed carbon electrode (SPCE) was investigated as a biosensor for the detection of nitrite based on its electrochemical and catalytic properties. CcR was covalently coupled with SAM layers on GNPs by using EDC and NHS. Direct electrochemical response of CcR biofunctionalized electrodes showed a couple of well-defined and nearly reversible cyclic voltammetric peaks at −0.34 and −0.45 *vs*. Ag/AgCl. Under optimal conditions, the biosensor could be used for the determination of NO_2^- with a linear range from 0.1–1600 μm and a detection limit of 60 nM with a sensitivity of 0.172 μA μM^{-1} cm^{-2}. Further, we have designed and developed a novel and cost effective portable electrochemical analyzer for the measurement of NO_2^- in hypoxia induced H9c2 cardiac cells using ARM microcontroller. The results obtained here using the developed portable electrochemical nitrite analyzer were also compared with the standard cyclic voltammetry instrument and found in agreement with each other.

1. Introduction

Nitrite (NO_2^-) is a central homeostatic molecule in nitric oxide (NO) biology and serves as an important signaling molecule in its own right (Bryan, 2006; Bryan and Matthew, 2007) and also has a protective role against ischemia/reperfusion injury (Bryan et al., 2007; Raat et al., 2009; Shiva and Gladwin, 2009). Nitrite supplementation limits hypoxia-induced oxidative stress and activates the alternate nitrite-NO-cGMP pathway which may partially account for the nitrite-mediated cardioprotection. Moreover, nitrite supplementation also regulates HIF-1α stability during hypoxia and subsequent hypoxia responsive gene expression (Manjulata et al., 2012). It also extends the role of nitrite in modulating expression of genes, transcription factors and signaling networks during hypoxia supporting the signaling potentials of nitrite (Ernst et al., 2009). Further, NO_2^- is also effective in inhibiting mitochondrial respiration (Shiva et al., 2007), and regulating expression of gene and protein during pathophysiological range of oxygen tension (Duranski et al., 2005; Perlman et al., 2009). Recent and past studies have shown that NO_2^- exerts different effects on the cell machinery leading to cell death, apoptosis and/or necrosis both *in vivo* and *in vitro* (Catherine et al., 2002; Sruti, 2010).

Dysfunction of cardiac energy metabolism plays a critical role in many cardiac diseases, including heart failure (Doenst et al., 2013), myocardial infarction (Turer and Hill, 2010), ischemia–reperfusion injury (Engel et al., 2006) and organ transplantation (Theodore et al., 2012; Kuznetsov et al., 2015). H9c2 cells were found to be closer to normal primary cardiomyocytes with regard to their energy metabolism features. Like primary cardiomyocytes, they are more sensitive to

* Corresponding author.
E-mail address: ckarunakaran2000@gmail.com (C. Karunakaran).

http://dx.doi.org/10.1016/j.bios.2016.10.039
Received 2 August 2016; Received in revised form 6 October 2016; Accepted 18 October 2016
Available online 19 October 2016
0956-5663/

hypoxia than HL1 cells and, therefore, can be more suitable in the design of the *in vitro* model of cardiac hypoxia reoxygenation, myocardial infarction and other related diseases (Andrey et al., 2015). For these reasons, in our experiment we used embryonic rat heart-derived H9c2 cardiomyoblasts cells for measuring nitrite levels under normaxia and hypoxia conditions.

The electrochemical determination of NO_2^- as well as its interaction with iron proteins has attracted considerable attention. Numerous examples of NO_2^- biosensors can be found in the literature, either using nonspecific proteins *viz*. hemoglobin (Jianmin and Zhihui, 2009; Zhang and Yi, 2009), and cytochrome *c* (Chen et al., 2009) or employing selective NO_2^- reducing enzymes, namely the multi-hemic cytochrome *c* nitrite reductase (ccNiR) (Zhang et al., 2009), and cytochrome-cd1 nitrite reductase (cyt-cd1 NiR) (Strehlitz et al., 1996; Almeida et al., 2010; Celia et al., 2010; Célia et al., 2015). Cytochrome *c* reductase (CcR), an another heme protein, is one of the three major respiratory enzyme complexes residing in the inner mitochondrial membrane of all animals and all aerobic eukaryotes and most eubacteria (Zhang et al., 1998; Hunte et al., 2003; Crofts, 2004). Further, CcR is a redox protein participating in the mitochondrial electron transport redox reactions and this may play a role in metabolizing NO_2^- in mitochondria. So, we have attempted here to examine its electrocatalytic properties for NO_2^- determination.

Recently, electrochemical determination of various electroactive substrates using cyclic voltammetry (CV) and amperometry have been reported (Rajesh et al., 2010; Pandiaraj et al., 2013; Pandiaraj et al., 20142014a; Madasamy et al., 2014). However, the physical instrument having these techniques involves high cost and the hardware instrumentation systems are made up of pre-defined hardware components that are completely specific to their measurement function (Karunakaran et al., 2014). Because of their hard-coded function, these stand-alone physical instruments are more limited in their versatility (Madasamy et al., 2012; Tian et al., 2016). Therefore, the development of hand-held, inexpensive and easy to use analytical assays for the measurement of NO_2^- has been the focus of intensive research efforts. The recent development of software and hardware technology opens a new way to overcome these drawbacks with the help of microcontroller based portable devices (Dogo et al., 2013; Anju Latha et al., 2012; Arun Venkatesh et al., 2015). Several groups have designed and fabricated microcontroller based potentiostats for electrochemical biosensing application (Pandiaraj et al., 20142014b; Loncaric et al., 2012; Shi et al., 2008).

Amperometric based electrochemical analyzers have also been widely reported for the detection of glucose and ascorbic acid (Beni et al., 2015; Elias et al., 2005; Sangam and Patre, 2009; Serra et al., 2007). In addition, the design of electrochemical analyzers performing CV for the detection of cytochrome c, glucose and lyzozyme also reported (Pandiaraj et al., 20142014b; Loncaric et al., 2012; Kwakye and Baeumner, 2007). Moreover, in most of the designs the data transfer and storage were done by interfacing of microcontroller with PC through an RS-232 connection or USB interface. The main disadvantages of these devices are that they need PC for monitoring and data logging (Huang et al., 2009; Laguarda-Miro et al., 2012). Also, the prototype instrumentations for biosensing applications have used PIC8F4550 and AT89C51 microcontrollers (Pandiaraj et al., 20142014b; Loncaric et al., 2012; Sangam and Patre, 2009; Serra et al., 2007; Shiwani and Suri, 2010). These microcontrollers have 8 bit CPU, low RAM and limited capability. Due to this issue an ARM microcontroller based data acquisition system with data logger and display unit is proposed for the measurement of NO_2^-. It has salient futures such as 1 clock/instruction speed, 32 bit data bus width, 64 KB RAM, 512 KB ROM built-in ADC and operates at 3.3 V power consumption for fast processing and high end communication protocol.

In this work, we have combined the distinct advantages of ARM microcontroller based portable sensing device and covalently biofunctionalized CcR onto the SAM-GNP-PPy-SPCE system for the direct measurement of NO_2^- levels in cultured H9c2 cardiac cells under hypoxia condition. Further, in this approach, we have used CV based amperometric method in the electrochemical analyzer for accurate measurement of NO_2^- levels.

2. Experimental

2.1. Chemicals and reagents

Cytochrome c reductase from porcine heart (C3381), embryonic rat heart-derived H9c2 cardiomyoblasts (88092904), penicillin-streptomycin (P4333), Fetal Bovine Serum (FBS) (F2442), pyrrole, potassium chloride, sodium dihydrogen phosphate, disodium hydrogen phosphate, sodium nitrite, sodium nitrate, auric chloride trihydrate, N-(3-dimethylaminopropyl)-N′-ethylcarbodiimide hydrochloride (EDC), N-hydroxysuccinimide (NHS), 11-mercaptoundecanoic acid (11-MUA), 2-mercaptoethanol (2-ME), diethylenetriaminepentaacetic acid (DTPA), glucose (D7777), Trypsin-EDTA (T9049) were purchased from Sigma Aldrich (USA). All the reagents were prepared by using doubly distilled water.

2.2. Instruments

The morphological changes of the modified electrodes were obtained using FEI Quanta FEG High Resolution scanning electron microscope (SEM) (FEI Co., Netherlands). All cyclic voltammetric experiments were measured using CHI 1200B electrochemical workstation (CHI, USA). Screen printing carbon electrode assemblies for constructing the sensor were obtained from Zensor R & D, Taiwan consisting of carbon working, carbon counter and an Ag/AgCl reference electrode.

2.3. Fabrication of CcR biofunctionalized SAM-GNP-PPy-SPCE

The overall scheme of fabrication process of CcR biofunctionalized electrode is shown in Fig. 1. The modification of GNP onto PPy modified SPCE was fabricated as per our previous reports (Pandiaraj et al., 20142014a; Santharaman et al., 2016). After GNP coverage on PPy-SPCE, SAM layer was formed on that surface by using equimolar mixture of 5 mM 11-MUA and 2-ME for 24 h for CcR immobilization. Finally covalent immobilization of CcR enzyme was realized by means of EDC and NHS (Cortina-Puig et al., 2009; Li et al., 2007; David and Joseph, 2003). The SAM monolayer on the surface of GNP-PPy-SPCE was activated by rinsing the electrode with phosphate buffer and with 5 μL of a mixture containing EDC (200 mM) and NHS (50 mM) in water for about 10 min. After removing EDC-NHS mixture, the surface of the working electrode was rinsed with 0.1 M PBS buffer solution (pH 7.0). The CcR biofunctionalization was carried out by dropping 5 μL of CcR solution (25 U/ml) onto the surface of SAM-GNP-PPy-SPCE for 24 h. Then, these electrodes were treated with 0.1 M PBS to remove any electrostatically adsorbed CcR proteins and rinsed with the water before use. In addition, CcR-PPy-SPCE was prepared to study the effect of nanoparticles on the biosensor surface by using the same procedure described above except GNP-SAM formation.

2.4. Portable electrochemical device description

A microcontroller based data acquisition unit integrated with potentiostat circuit capable of performing CV coupled amperometric technique is used for the analysis. The acquired biosensor data were processed into digital form by the microcontroller for analysis. Graphical user interface (GUI) a user friendly software based system implemented here makes the analyzer easy to operate. We have designed and programmed the portable electrochemical analyzer based on three electrode setup to perform CV and amperometry for NO_2^- determination. Since, CV is a very important electrochemical technique

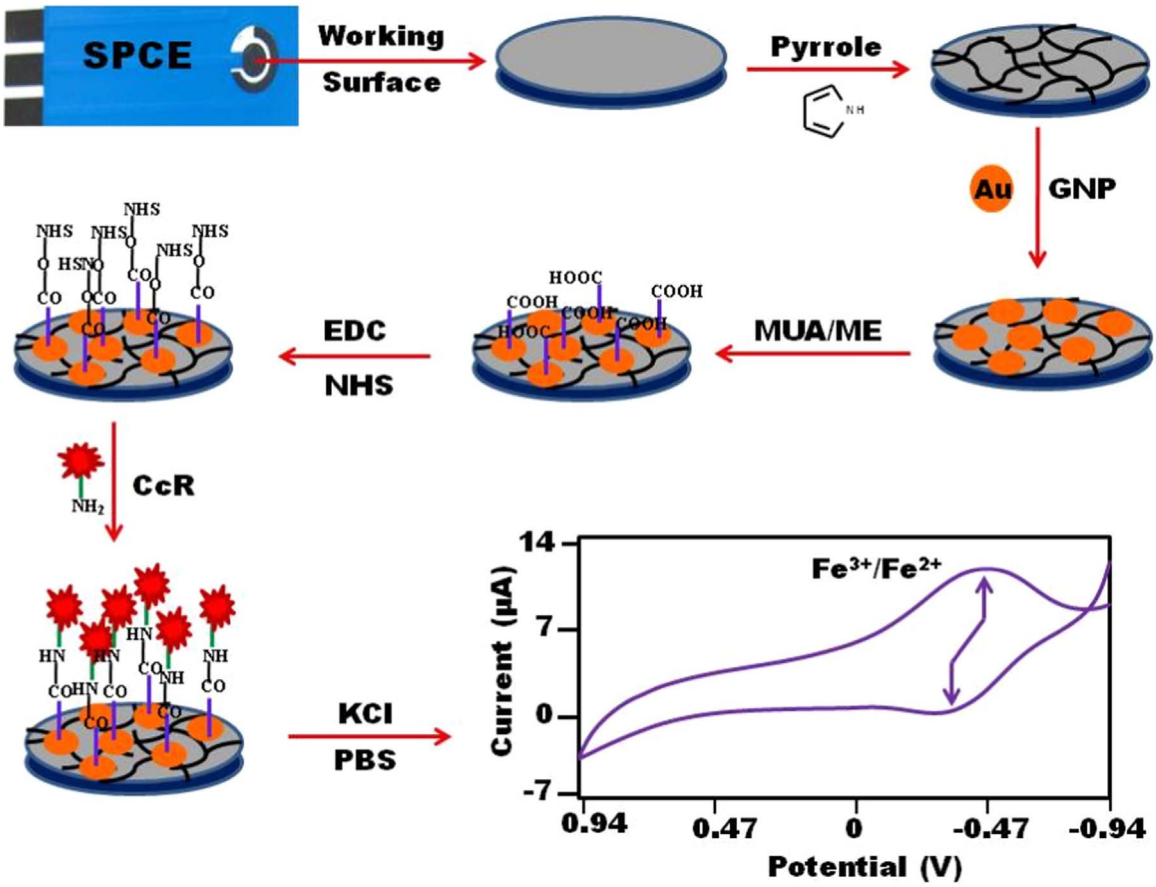

Fig. 1. Schematic representation of the step-wise fabrication of nitrite biosensor using CcR immobilized onto miniaturized disposable screen printed carbon electrode.

used to study the mechanism of charge transfer reaction of redox species, in particular to determine the concentration of various analytes present in industry, medical and biological samples etc, based on different chemical or biosensors using their redox behavior. Similarly, amperometric method is used to study the presence of ion in solution on the basis of change in current (Wang, 2000; Nicholson and Shain, 1964; Mundinamani and Rabinal, 2014; Bard and Faulkner, 2001). In CV, the biasing voltage across the working and reference electrodes linearly swept, while the resultant current across the working and counter electrodes measured throughout the electrochemical process in a three electrode type design. Further, the change in current corresponding to concentration was measured using amperometrically.

2.5. Circuit design, hardware and software descriptions

The overall circuit diagram of the microcontroller based portable cyclic voltammetric analyzer for NO_2^- is shown in Fig. 2. A miniaturized three electrode system was connected to an ARM CORTEX M3 (LPC1768) microcontroller based data acquisition unit containing home-made potentiostat circuit, a level shifter, and an op-amp inverter (TL084). The necessary voltammetric waveform between the specified voltage ranges to be applied to the electrodes was produced by the built-in 12-bit digital to analog converter (DAC) of the LPC1768 microcontroller. The output current generated at the working electrode (WE) as a result of electrochemical reaction was converted to voltage using a current to voltage (I/V) converter and measured using an in-built analog to digital converter (ADC) of the microcontroller.

The ARM microcontroller has an in-built 12-bit ADC. Since the microcontroller can only accept the positive voltages, the output voltage is level shifted by using an op-amp TL084 to accommodate negative voltages. Microcontroller sends the analog sweep voltage value to the potentiostat through the built-in DAC. Output voltage from the potentiostat circuit was fed to the ADC of the microcontroller. The data was processed by the microcontroller and stored the measurement data in an EEPROM (AT24LC04) and displayed the data in TFT (Thin-film transistor; 320×480 high resolution) display. Switches were used to enter the range and select the calibration mode. The firmware program has been developed in 'C' using IAR Embedded Workbench. The written software program as given in Supplementary Information is used to perform and control all the electrochemical analyzer functions.

2.6. H9c2 cardiomyoblasts cell culture

Embryonic rat heart-derived H9c2 cardiomyoblasts were cultured in Dulbecco's modified Eagle's medium (DMEM) with high glucose. The media was supplemented with Penicillin-Streptomycin and 10% fetal bovine serum (FBS) in a humidified CO_2 incubator with 5% CO_2 maintained at 37 °C (Andrey et al., 2015; Duan et al., 2016). Cells were sub-cultured routinely at a confluency of 70–80% and harvested using Trypsin-EDTA. For the experiment, cells were seeded at a density of 30% in 60 mm dish and allowed to reach a confluency of 60–70% prior to the treatment. Cells were then shifted to fresh growth media and stimulated as defined below. The cells were harvested using Trypsin-EDTA post-exposure and washed with 1X PBS (1500 rpm, 10 min, and 4 °C).

3. Results and discussion

3.1. Scanning electron microscopic characterization of modified electrodes

The morphological changes of each modification of the SPCE-based

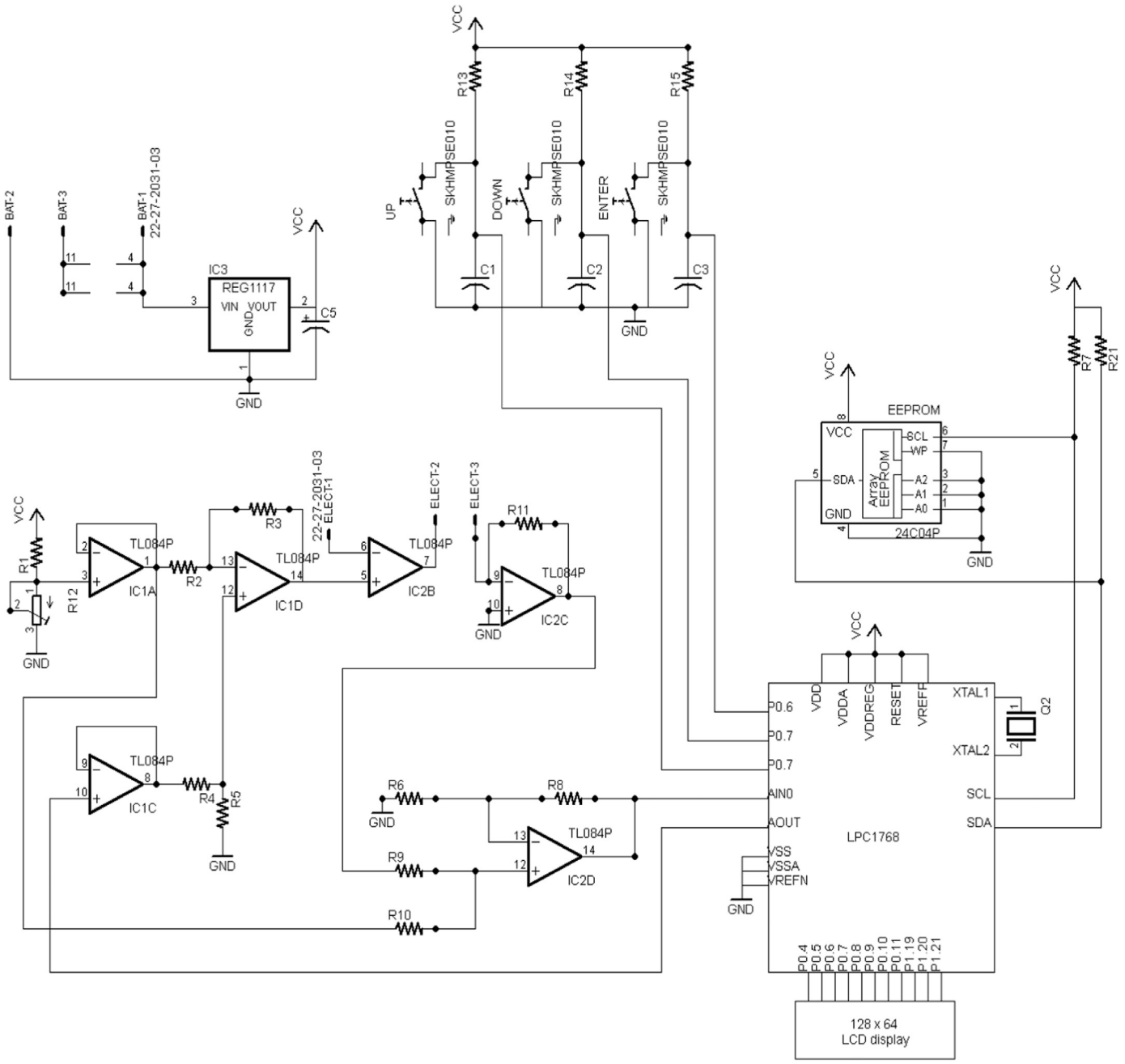

Fig. 2. Circuit diagram of the portable ARM CORTEX M3 microcontroller based electrochemical nitrite analyzer.

biosensor during fabrication process were monitored by using scanning electron microscopy (SEM). Fig. 3a, b and c illustrate the SEM images of bare SPCE, PPy-SPCE and GNP-PPy-SPCE electrodes respectively. Fig. 3a shows the homogenous bare surface of the SPCE while, Fig. 3b reveals the distinctive highly porous surface morphology of PPy on SPCE. Consequently the porous and thereby high surface area nature of the PPy provides more sites for subsequent GNP and CcR immobilization than the bare SPCE alone. Further, SEM reveals a uniform distribution of GNPs with average diameter of ~25 nm and moderately symmetric distribution over the microporous matrix of the PPy-SPCE (Fig. 3c) (Pandiaraj et al., 20142014a). This GNP nanostructured surface also enables more immobilization of SAM molecules by providing a large surface area for CcR as biorecognition agent binding. Moreover, after the electrodeposition of GNPs onto the PPy-SPCE, it showed a characteristic cathodic peak at +0.28 V for Au (data not shown here) in 0.1 M PBS (Pandiaraj et al., 20142014a; Santharaman et al., 2016), confirming the successful coating of GNPs onto the PPy-SPCE.

3.2. The voltammetric characterization of modified biosensors

Cyclic voltammetry experiments were performed to analyze the electrochemical characteristics of the conducting surface of SPCE after each electrode modification step and further confirm the immobilization of CcR protein moieties. Fig. 4 shows the typical CVs of CcR-SAM-GNP-PPy-SPCE (curve d), SAM-GNP-PPy-SPCE (curve c), PPy-SPCE (curve b), and SPCE (curve a) electrodes in the presence of 0.1 M PBS (pH 7.0) containing 0.1 M KCl as a supporting electrolyte at a scan rate of 50 mVs^{-1}. There were no considerable redox peaks obtained for bare SPCE (curve 4a), PPy-SPCE (curve 4b) and SAM-GNP-PPy-SPCE (curve 4c) in the specified voltage range, indicating no Faradaic electron transfer process occurs. Further, after the biofunctionalization

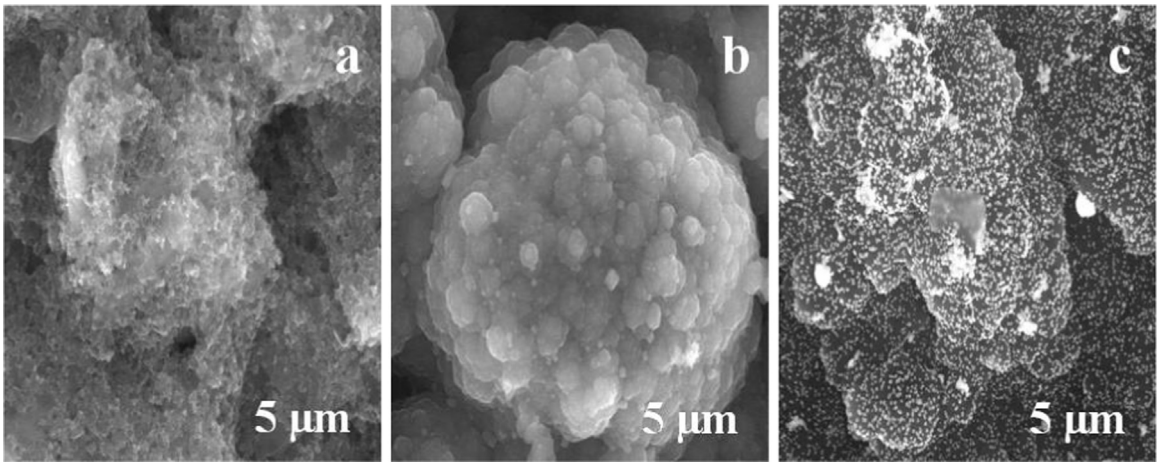

Fig. 3. SEM images of bare SPCE (a), PPy functionalized SPCE (b) and GNP incorporated PPy/SPCE (c) surfaces.

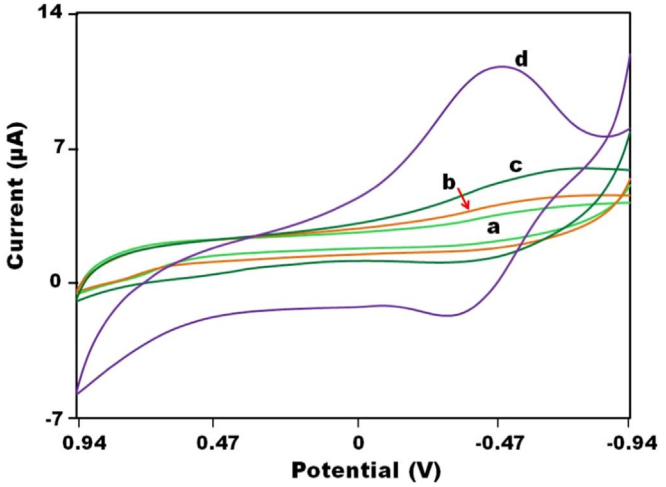

Fig. 4. Typical cyclic voltammetric responses of (a) bare SPCE, (b) PPy-SPCE, (c) SAM-GNP-PPy-SPCE and (d) CcR-SAM-GNP-PPy-SPCE electrodes in 0.1 M PBS (pH 7.0) containing 100 µm DTPA in 0.1 M KCl using the scan rate of 50 mVs^{-1} *vs.* Ag/AgCl.

of CcR on SAM-GNP-PPy-SPCE (curve 4d), a pair of characteristic reversible redox peaks at −0.34 and −0.45 V *vs.* Ag/AgCl (Pandiaraj et al., 2013) was observed. These Faradaic redox peaks clearly attributed to the electron transfer between the Fe(III)/Fe(II) redox couple of the CcR and the nanocomposite modified electrode surface. Hence, it clearly reveals that the CcR was covalently coupled on SAM-GNP-PPy nanocomposite modified electrode surface *via* EDC and NHS. The optimization processes *viz.* effect of pH and effect of scan rate were studied and given in Supplementary Information.

3.3. Electrochemical response to NO_2^-

Fig. S3 explains the electrochemical responses obtained for the CcR-PPy-SPCE and CcR-SAM-GNP-PPy-SPCE in the absence (curve a & curve b) and presence (curve c & curve d) of 100 µm NO_2^- using a scan rate of 50 mVs^{-1} containing 100 µm DTPA in 0.1 M KCl solution. Before the addition of NO_2^-, there were no changes observed in the current response. However, after the addition of 500 µm NO_2^-, both the CcR-PPy-SPCE and CcR-SAM-GNP-PPy-SPCE exhibited an increase in current anodically at the potential of +0.8 V (Madasamy et al., 2014). It is ascribed to the electrochemical oxidation of NO_2^- to NO_3^- *via* an active site Fe(III/II) in the CcR moiety. Further, it is obviously seen that the CcR-SAM-GNP-PPy-SPCE electrode (Fig. S3, curve d) shows significantly higher current than CcR-PPy-SPCE (Fig. S3, curve c). It is perhaps due to the additional surface area provided by the GNP-PPy nanocomposite enhancing the immobilization of CcR as well as accelerating electron transfer between underlying electrode and the active site of CcR. This is because of GNPs greatly facilitated and provided its surface to covalent coupling with CcR.

The electrochemical responses of the CcR-SAM-GNP-PPy-SPCE electrode in 0.1 M PBS (control) and various concentrations of NO_2^- using the scan rate of 50 mVs^{-1} are shown in Fig. 5. As the concentration increases, the anodic current response is also increased linearly at 0.8 V as a characteristic potential for NO_2^- determination (Madasamy et al., 2014). Inset Fig. 5 represents the plot of observed anodic peak currents against NO_2^- concentrations. The calibration curve thus obtained exhibits a linear range of response over the concentration of NO_2^- from 100 nM to 1600 µm but for clarity here we have shown from 50 µm to 1600 µm (r^2 =0.998 and n =3) with a detection limit of 60 nM and the sensitivity of 0.172 µA μM^{-1} cm^{-2} for CcR biosensor. Further, the analytical characteristics such as sensitivity, linear range and detection limit of the present biosensor were compared with the earlier reported NO_2^- biosensors (Table S1).

3.4. Analytical performance of the ARM based NO_2^- analyzer

The electrocatalytic activity of the CcR-SAM-GNP-PPy-SPCE biosensor toward the determination of NO_2^- was assessed by the developed portable low-cost electrochemical analyzer. The accuracy of the

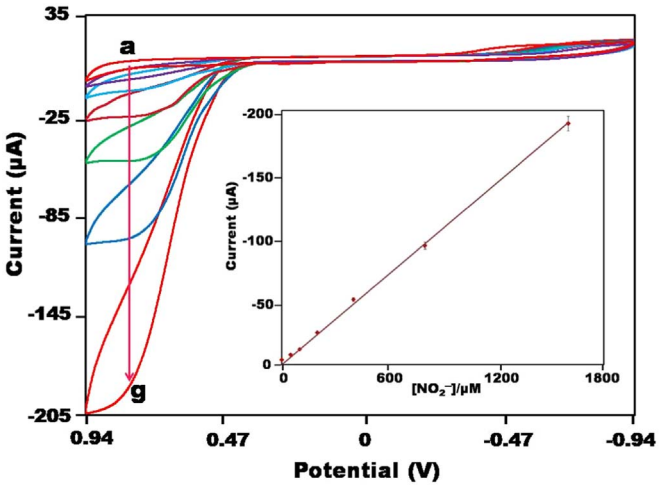

Fig. 5. The electrochemical responses of the CcR-SAM-GNP-PPy-SPCE electrode in (a) 0.1 M PBS, (b) 50 µm, (c) 100 µm, (d) 200 µm, (e) 400 µm, (f) 800 µm and (g) 1600 µm of NO_2^- solution using the scan rate of 50 mVs^{-1} *vs.* Ag/AgCl. Inset figure represents the linear calibration plot of anodic peak currents against NO_2^- concentrations (y=−0.119x-4.2, r^2=0.998). Each point represents the average of three measurements.

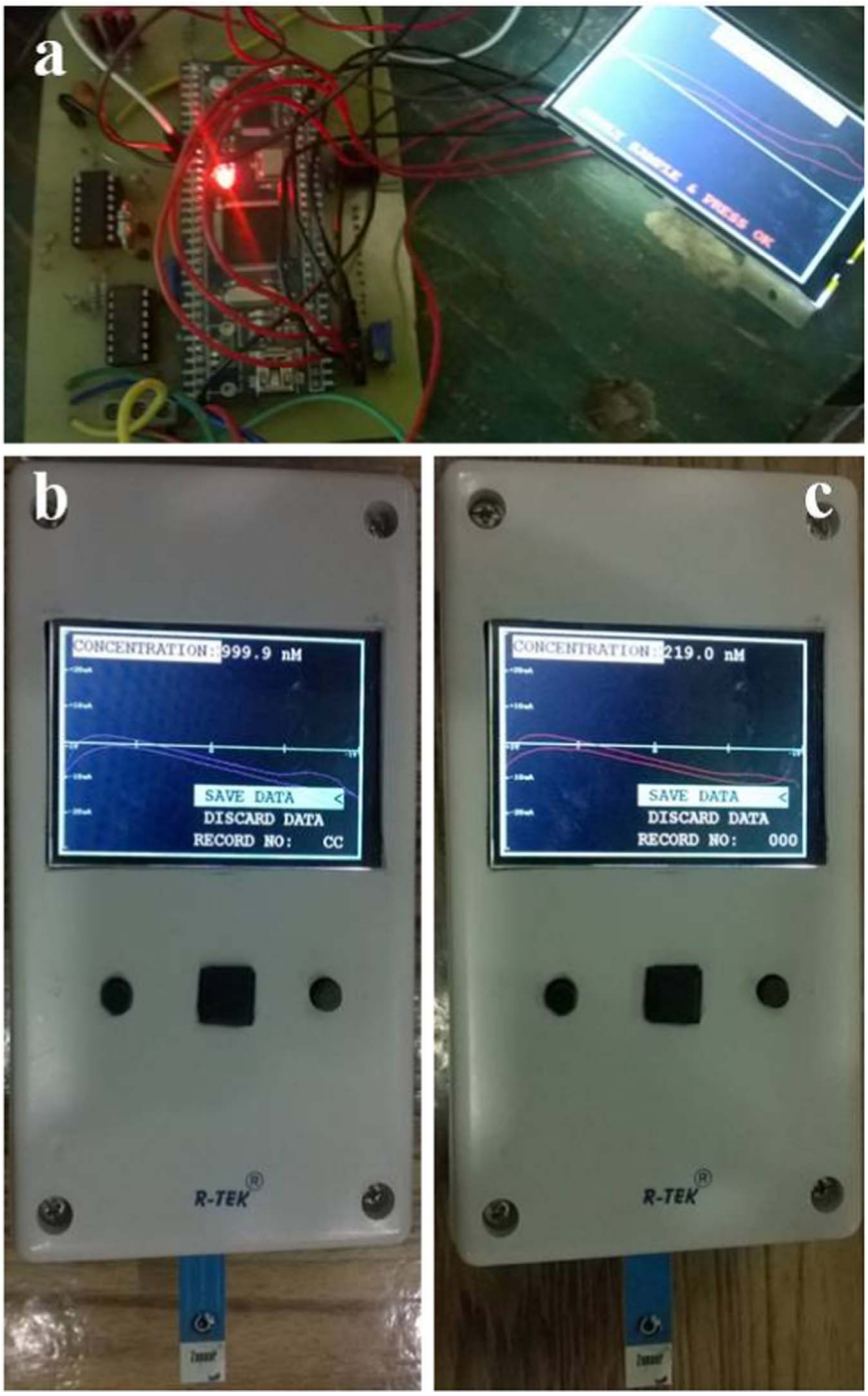

Fig. 6. Pictures of (a) actual physical appearance of portable ARM CORTEX M3 microcontroller based electrochemical analyzer using low power 320×480 pixels multi color TFT LCD display showing the biosensor response of CcR peak in 0.1 M PBS containing 0.1 M KCl, (b) Experimental verification of electrochemical analyzer using the CcR biosensor at 1 μm NO_2^- concentration, (c) Measurement of NO_2^- in supernatant of hypoxia induced H9c2 cell lysate (0.1% O_2 for 48 h).

developed instrument was evaluated by comparing its results with that of a commercial electrochemical analyzer (CHI1200B) under same experimental conditions. Fig. 6a shows the photograph of an inner circuit and the electrochemical CV response obtained for the CcR-SAM-GNP-PPy-SPCE using the developed portable electrochemical analyzer in the presence of 0.1 M PBS in 0.1 M KCl. The portable analyzer swept the voltage from −1 to +1 V and stored the values of current produced by the sensor at 0.8 V and those values were processed amperometrically and displayed in the TFT display for different concentrations. The calibration option was selected for the first time; a sensor under test has connected with the system. Known values of NO_2^- concentrations were applied over the biosensor surface and both cyclic and amperometric calibration measurements were done. After the completion of measurements, the data were stored in the EEPROM. The system was battery operated and the battery voltage was monitored by the microcontroller (see Fig. S4). The resistance fixed in this circuit (1 MΩ) is suitable for low concentrations and current values. Fig. 6b shows the photograph of complete device of LPC1768 microcontroller based electrochemical nitrite analyzer for the measurement of standard 1000 nM NO_2^- solution. It clearly reveals that the combination of the developed portable analyzer and CcR based biosensor is suitable for point-of-care applications for NO_2^- determination.

3.5. Measurement of NO_2^- in hypoxia induced cardiac cell lines

In order to further investigate the feasibility of the newly developed CcR based biosensor for clinical analysis, NO_2^- levels were measured in H9c2 cells by using the biosensor and also the reference kit (Measure iT- high-sensitivity nitrite assay kit, Molecular Probes, Eugene, OR, USA) according to manufacturer's instructions. Exposure of H9c2 cells to hypoxia induces stress and reportedly alters the biomarkers level (Kai et al., 2015; Russell et al., 2003). Hence, H9c2 cells cultured either at normoxia (CO_2 incubator maintained at 5% CO_2, 95% air and 37 °C), or hypoxia (CO_2 incubator maintained at 5% CO_2, 0.1% O_2 and 37 °C) for 24 h (Hypoxia I) and 48 h (Hypoxia II). The cells were seeded at a density of 30% in 60 mm culture dish and allowed to reach a confluency of 60–70% prior to the treatment. Cells were then transferred to fresh growth media and cultured under hypoxia conditions mentioned above. Post hypoxia exposure, both the normoxic and hypoxic cells were harvested using Trypsin-EDTA post-exposure and washed with 1X PBS (1500 rpm, 10 min, and 4 °C). The cell pellet was re-suspended in RIPA buffer containing protease inhibitor cocktail. The total protein was extracted by lysis in RIPA buffer (incubation on ice 25–30 min with intermittent tapping, then spun, at 10000 rpm for 15 min at 4 °C). Then, the supernatant of cell lysate was aliquoted for the analysis using biosensor as well as nitrite estimation kit and kept in ice during analysis.

The measurements of NO_2^- levels were performed on the normaxia and hypoxia induced H9c2 cells using cellulose acetate (CA) membrane coated CcR-SAM-GNP-PPy-SPCE biosensor and reference kit. Earlier, it has been reported that CA membrane was perm selective for NO_2^- and NO_3^- (Madasamy et al., 2014; Badea et al., 2001). In order to eliminate all the possible interferences (see Supplementary Information), CA membrane was coated onto the CcR-SAM-GNP-PPy-SPCE by dropping 10 µL of CA solution (2 g of cellulose acetate and 20 mg of polyvinyl acetate in 30 ml acetone and 20 ml cyclohexanone) and dried at room temperature for 10 min (Célia et al., 2015; David and Joseph, 2003). After that, the concentration of NO_2^- was measured and calculated by interpolating the obtained current response onto the calibration plot prepared by the NO_2^- standard solutions. Each reading represents the average of three measurements. Moreover, the measured values were validated by comparing the results obtained using high-sensitivity reference nitrite assay kit. The NO_2^- levels present in supernatant of H9c2 cell lysates were obtained using the CcR biosensor connected to standard CV instrument under normoxia (65 ± 20 nM), hypoxia I (156 ± 22 nM) and hypoxia II (235 ± 26 nM). These observations were found to be comparable with the NO_2^- estimation by using reference kit (68 ± 17; 162 ± 28; 229 ± 23 nM for normoxia, hypoxia I and hypoxia II respectively). These results therefore confirmed the suitability of the electrode for the measurement of cellular NO_2^- levels. In addition, the NO_2^- levels in hypoxia induced H9c2 cells measured using the CcR biosensor interfaced LPC1768 electrochemical analyzer shows a comparable analytical performance. The values obtained from portable device (66 ± 15; 167 ± 19; 219 ± 20 nM for normoxia, hypoxia I and hypoxia II respectively) were well correlated with the standard CV instrument and reference assay. Fig. 6c shows the photograph of the measurement of NO_2^- in H9c2 cells under 0.1% O_2 for 48 h (hypoxia II) by using the portable analyzer.

3.6. Stability and reproducibility of the constructed NO_2^- biosensors

The fabrication reproducibility of five electrodes of CcR, made independently, showed an acceptable reproducibility with a R.S.D.s of 3.8% for the current determined at a NO_2^- concentration of 100 µm respectively. Thus, CcR-SAM-GNP-PPy-SPCE electrodes were very efficient retaining the electrocatalytic activity of Fe(III)/Fe(II) redox couple and preventing CcR from leaking out of the sensor surface.

The storage stabilities of NO_2^- biosensor based on CcR stored in air at 4 °C were examined by checking periodically their relative response currents (the ratios of the catalytic currents detected at different times to the initial current value) in 0.1 M PBS (pH 7.0) containing 100 µm NO_2^-. The CcR shows its maximum activity (98%) upto 3 weeks without losing its activity. After a storage period of 5 weeks at 4 °C the CcR biosensor showed on 12% loss of activity for NO_2^-. However, after 5 weeks the activity of CcR-SAM-GNP-PPy-SPCE was fall down slowly and exhibited 55% activity after two months. Thus, the biosensors were stored in air at 4 °C when not in use.

4. Conclusion

Cytochrome c reductase has been effectively conjugated to SAM-GNP-PPy nanomatrix onto the SPCE by a covalent coupling method using EDC and NHS. The GNP-PPy nanostructure provided a microenvironment around the protein to retain its enzymatic bioactivity. The immobilized CcR displayed a fast direct electron transfer and a good electrocatalytic response to nitrite. The biosensor showed a wide linear range, low detection limit, good reproducibility and stability. Also, the development of portable ARM CORTEX M3 microcontroller based electroanalytical instrument performing by the combination of cyclic voltammetry and amperometric techniques for the determination of NO_2^- has been presented. Further, the constructed biosensor based measurements for biological samples were in accordance with the standard high-sensitivity nitrite assay kit. Moreover, the results obtained from the developed analyzer were well correlated with the standard device. Thus, the bioconjugated CcR and ARM microcontroller based electrochemical nitrite analyzer provided an enhanced stability, efficient strategy and a new promising way for nitrite determination in biological samples and the development of point-of-care applications.

Acknowledgments

This work was supported by the Defence Institute of Physiology & Allied Sciences (DIPAS), Defence Research and Development Organisation (DRDO), Delhi, India (TC/370/TASK-191 (CK)/DIPAS/2013) and the Managing Board of Virudhunagar Hindu Nadar's Senthikumara Nadar College (Autonomous), Virudhunagar, Tamil Nadu, India.

Appendix A. Supplementary material

Supplementary data associated with this article can be found in the online version at doi:10.1016/j.bios.2016.10.039.

References

Almeida, M.G., Serra, A., Silveira, C.M., Moura, J.J.G., 2010. Sensors 10 (12), 11531–11535.
Andrey, V.K., Sabzali, J., Stephan, S., Sandra, F., Michael, G., 2015. Biochim. Biophys. Acta 1853 (2), 276–284.
Anju Latha, N., Rama Murthy, B., Sunitha, U., 2012. Int. J. Eng. Res. Appl. (IJERA) 2 (5), 1440–1444.
Arun Venkatesh, K., Benjamin, A.R., Karunakaran, C., Elango, S., 2015. Instrumentation. In: Karunakaran, C., Kalpana, B., Benjamin, A.R. (Eds.), Biosensors and Bioelectronics1st ed..
Badea, M., Amine, A., Palleschi, G., Moscone, D., Volpe, G., Curulli, A., 2001. J. Electroanal. Chem. 509 (2001), 66–72.
Bard, A.J., Faulkner, L.R., 2001. Electrochemical Methods: Fundamentals and Applications 2nd ed.. Wiley, New York.
Beni, V., Nilsson, D., Arven, P., Norberg, P., Gustafsson, G., Turner, A.P.F., 2015. ECS J. Solid State Sci. Technol. 4 (10), S3001–S3005.
Bryan, N.S., 2006. Free Radic. Biol. Med. 41 (5), 691–701.
Bryan, N.S., Matthew, B.G., 2007. Free Radic. Biol. Med. 43, 645–657.
Bryan, N.S., Calvert, J.W., Elrod, J.W., Gundewar, S., Ji, S.Y., Lefer, D.J., 2007. PNAS 104, 19144–19149.
Catherine, G., Ruben, M., Afshin, S., 2002. FASEB J., 135–146.
Celia, M.S., Sofia, P.G., Alberto, N.A., M. Conceicao, B.S.M.M., Smilja, T., Ana, S.V., Rui, J.C.S., Jose, J.G.M., Gabriela, A.M., 2010. Biosens. Bioelectron. 25, 2026–2032.
Célia, M.S., Pedro, O.Q., Isabel, M., José, J.G.M., Peter, H., Gabriela, A.M., Smilja, T.,

2015. PLoS One, 1–18.
Chen, Q., Ai, S., Zhu, X., Yin, H., Ma, Q., Qiu, Y., 2009. Biosens. Bioelectron. 15 (24(10)), 2991–2996.
Cortina-Puig, M., Muñoz-Berbel, X., Regis, R., Calas-Blanchard, C., Jean-Louis, M., 2009. Bioelectrochemistry 76, 76–80.
Crofts, A.R., 2004. Annu. Rev. Physiol. 66, 689–733.
David, L.C., Joseph, A.L., 2003. J. Electro. Chem. 553, 187–190.
Doenst, T., Nguyen, T.D., Abel, E.D., 2013. Circ. Res. 113 (6), 709–724.
Dogo, E.M., Sado, F., Adah, S.M., 2013. Afr. J. Comp. ICT 6 (5), 121–128.
Duan, L., Lei, H., Zhang, Y., Wan, B., Chang, J., Feng, Q., Huang, W., 2016. Cardiology 133, 44–53.
Duranski, M.R., Greer, J.J., Dejam, A., Jaganmohan, S., Hogg, N., Langston, W., Patel, R.P., Yet, S.F., Wang, X., Kevil, C.G., Gladwin, M.T., Lefer, D.J., 2005. J. Clin. Invest. 115, 1232–1240.
Elias, M.A., Mamas, I.P., Constantinos, E.E., 2005. Sens. Actuators B Chem. 107, 372–378.
Engel, F.B., Hsieh, P.C., Lee, R.T., 2006. Proc. Natl. Acad. Sci. USA 103, 15546–15551.
Ernst, E.F., Soheyl, B., Martin, F., Neil, H., Malte, K., Daniel, B.K.S., Andrey, V.K., Haitao, L., Jon, O.L., Ron, M., Hans, N., Tienush, R., Alexandre, S., Anny, S.S., Sruti, S., Anatoly, F.V., Eddie, W., Jay, Z., Mark, T.G., 2009. Med. Res. Rev. 29 (5), 683–741.
Huang, C.Y., Tsai, T.C., Thomas, J.L., Lee, M.H., Liu, B.D., Lin, H.Y., 2009. Biosens. Bioelectron. 24, 2611–2617.
Hunte, C., Palsdottir, H., Trumpower, B.L., 2003. FEBS Lett. 545 (1), 39–46.
Jianmin, H., Zhihui, D., 2009. Sens. Actuators B Chem. 140, 222–226.
Kai, L., Yong-Chun, C., Hong, Z., Xiao-Peng, L., Dong, Z., Ai-Li, W., Jian, J.L., Yue, T., 2015. PLoS One 10 (7), e0132402.
Karunakaran, C., Madasamy, T., Pandiaraj, M., Niroj, K. Sethy, Kalpana, B., 2014. Electrochemical Biosensors for Hypoxia Markers. Singh, S.B., Prabhakar, N.R., Pentyala, S.N., (Eds.), Translational Research in Environmental and Occupational Stress, 1st ed.
Kuznetsov, A.V., Javadov, S., Sickinger, S., Frotschnig, S., Grimm, M., 2015. Biochim. Biophys. Acta 1853 (2), 276–284.
Kwakye, S., Baeumner, A., 2007. Sens. Actuators B Chem. 123, 336–343.
Laguarda-Miro, N., Francesca, W.F., García-Breijo, E., Ibáñez-Civera, J., Gil-Sánchez, L., Garrigues-Baixauli, J., 2012. Sens. Actuators B Chem. 171, 528–536.
Li, D., He, Q., Cui, Y., Duan, L., Li, J., 2007. Biochem. Biophys. Res. Commun. 355 (2), 488–493.
Loncaric, C., Tang, Y., Ho, C., Parameswaran, M.A., Yu, H.Z., 2012. Sens. Actuators B Chem. 161, 908–913.
Madasamy, T., Pandiaraj, M., Balamurugan, M., Karnewar, S., Benjamin, A.R., Arun Venkatesh, K., Vairamani, K., Srigiridhar, K., Karunakaran, C., 2012. Talanta 100, 168–174.
Madasamy, T., Pandiaraj, M., Balamurugan, M., Kalpana, B., Niroj, K., Sethy, Karunakaran, C., 2014. Biosens. Bioelectron. 52, 209–215.
Manjulata, S., Aditya, A., Rajesh, K., Kalpana, B., Niroj, K.S., 2012. Nitric oxide 26, 61–73.
Mundinamani, S.P., Rabinal, M.K., 2014. IOSR J. Appl. Chem. 7 (9), 45–52.
Nicholson, R.S., Shain, I., 1964. Anal. Chem. 36, 706.
Pandiaraj, M., Madasamy, T., Paradesi, N.G., Balamurugan, M., Srigiridhar, K., Rao, V.K., Kalpana, B., Karunakaran, C., 2013. Bioelectrochemistry 91, 1–7.
Pandiaraj, M., Niroj, K.S., Kalpana, B., Vepa, K., Chandran, K., 2014a. Biosens. Bioelectron. 54, 115–121.
Pandiaraj, M., Benjamin, A.R., Madasamy, T., Vairamani, K., Arya, A., Sethy, Niroj K., Kalpana, B., Karunakaran, C., 2014b. Sens. Actuators A 220, 290–297.
Perlman, D.H., Bauer, S.M., Ashrafian, H., Bryan, N.S., Garcia-Saura, M.F., Lim, C.C., Fernandez, B.O., Infusini, G., McComb, M.E., Costello, C.E., Feelisch, M., 2009. Circ. Res. 104, 796–804.
Raat, N.J.H., Noguchi, A.C., Liu, V.B., Raghavachari, N., Liu, D., Xu, X., Shiva, S., Munson, P.J., Gladwin, M.T., 2009. Free Radic. Biol. Med. 47, 510–517.
Rajesh, S., Kanugula, A.K., Kalpana, B., Govindaswamy, I., Srigiridhar, K., Karunakaran, C., 2010. Biosens. Bioelectron. 26, 689–695.
Russell, M.C., Sofija, J., Grant, R.B., Anthony, M.D., Harish, L., Roland, H.W., Kevin, A.R., Douglas, J.R., Harri, J.R., Aleksandar, J., 2003. J. Biol. Chem. 278 (33), 31444–31455.
Sangam, V.G., Patre, B.M., 2009. J. Instrum. Soc. India 39, 30–34.
Santharaman, P., Das, M., Singh, S.K., Sethy, N.K., Kalpana, B., Claussen, J.C., Karunakarana, C., 2016. Sens. Actuators B 236, 546–553.
Serra, P.A., Rocchitta, G., Bazzu, G., Manca, A., Puggioni, G.M., Lowry, J.P., Robert, D., 2007. Sens. Actuators B Chem. 122, 118–126.
Shi, Y., Dou, H., Zhou, A., Chen, Y., 2008. Sens. Actuators B Chem. 131, 516–524.
Shiva, S., Gladwin, M.T., 2009. Basic Res. Cardiol. 104, 13–19.
Shiva, S., Huang, Z., Grubina, R., Sun, J., Ringwood, L.A., MacArthur, P.H., Xu, X., Murphy, E., Darley-Usmar, V.M., Gladwin, M.T., 2007. Circ. Res. 100, 654–661.
Shiwani, S., Suri, C.R., 2010. Int. J. Comp. Appl. 6 (1), 21–27.
Sruti, S., 2010. Nitric Oxide 22 (2), 64–74.
Strehlitz, B., Gründig, B., Schumacher, W., Kronack, P.M.H., Vorlop, K.D., Kotte, H., 1996. Anal. Chem. 68, 807–816.
Theodore, K., Christopher, P.B., Maike, K., Ronald, J.K., 2012. Int. Rev. Cell Mol. Biol. 298, 229–317.
Tian, T., Jiuxing, L., Yanling, S., Leiji, Z., Zhi, Z., Chaoyong, J.Y., 2016. Lab. Chip 16, 1139–1151.
Turer, A.T., Hill, J.A., 2010. Am. J. Cardiol. 106, (360-36).
Wang, J., 2000. Analytical Electrochemistry. John Wiley & Sons, Inc., Hoboken, New Jersey, (Chapter 2).
Zhang, L., Yi, M., 2009. Bioprocess Biosyst. Eng. 32, 485–492.
Zhang, Z., Huang, L., Shulmeister, V.M., Chi, Y.I., Kim, K.K., Hung, L.W., Crofts, A.R., Berry, E.A., Kim, S.H., 1998. Nature 392 (6677), 677–684.
Zhang, Z., Xia, S., Leonard, D., Jaffrezic-Renault, N., Zhang, J., Bessueille, F., Goepfert, Y., Wang, X., Chen, L., Zhu, Z., Zhao, J., Almeida, M.G., Silveira, C.M., 2009. Biosens. Bioelectron. 15 (24(6)), 1574–1579.